forests

Article

Comprehensive Evaluation of Germplasm Resources in Various Goji Cultivars Based on Leaf Anatomical Traits

Zijun Yang [1], Guoli Dai [2], Ken Qin [2], Jiali Wu [1], Zhonghua Wang [1] and Cuiping Wang [1,3,*]

[1] School of Biological Science and Engineering, North Minzu University, Yinchuan 750021, China; 20237628@stu.nun.edu.cn (Z.Y.)
[2] National Wolfberry Engineering Research Center, Ningxia Academy of Agriculture and Forestry Sciences, Yinchuan 750002, China
[3] Ningxia Grape and Wine Innovation Center, North Minzu University, Yinchuan 750021, China
* Correspondence: wangcuiping@nmu.edu.cn

Abstract: The leaf is a critical organ for assimilation in plants, and the anatomical structure of the leaf can reflect the adaptability of plants to their environment to a certain extent. The research objects in this investigation were 36 different cultivars (lines) of goji germplasm resources. The structure and stoma condition of healthy leaves were the subject of a comparative investigation. Significant variations in leaf structural indices and stoma were identified among various goji cultivars (lines). The leaves of goji were the thickest and possessed the lowest stoma density. The resilience of goji germplasm resources was assessed using the main component analysis approach and the membership function. The results showed that LR (*L. ruthenicum* Murr.) and LCy (*L. cylindricum* Kuang) exhibited the strongest resistance. Goji resistance is significantly influenced by thickness of the upper cuticle (TUC) and thickness of the lower cuticle (TLC), according to the analytical results for several leaf anatomical indicators and stress resistance. By analyzing the wax content of 13 different goji cultivars (lines) and field infection results, it was found that Tianjing 3 had the highest wax content, the smallest average number of galls, and the smallest infection area. This suggests that Tianjing 3 has the strongest resistance to *Aceria pallida*, and that its insect resistance is correlated with its wax content. This study offers a thorough assessment of 36 goji germplasm resources' resilience, providing a point of reference for the selection and propagation of resistant cultivars within these resources.

Keywords: goji; anatomical traits; germplasm resources; evaluation

check for updates

Academic Editor: Ivar Wendling

Received: 3 December 2024
Revised: 9 January 2025
Accepted: 15 January 2025
Published: 20 January 2025

Citation: Yang, Z.; Dai, G.; Qin, K.; Wu, J.; Wang, Z.; Wang, C. Comprehensive Evaluation of Germplasm Resources in Various Goji Cultivars Based on Leaf Anatomical Traits. *Forests* **2025**, *16*, 187. https://doi.org/10.3390/f16010187

1. Introduction

Goji is a perennial woody species belonging to the *Lycium* genus within the Solanaceae family. It is predominantly found in temperate and subtropical regions, with a widespread distribution across a vast area of Asia, Africa, and the Americas. Goji is salt- and alkali-tolerant and thrives in poor soil, making it one of the key species for ecological construction in the arid northwest of China. It is extensively cultivated over large areas in provinces such as Ningxia, Gansu, Xinjiang, Qinghai, and Inner Mongolia, and is a significant economic crop in the dry regions of northwestern China [1–3]. Goji is rich in nutrients, containing abundant amounts of goji polysaccharides, flavonoids, and betaine, among other active components. It offers a variety of benefits, including enhancing immunity, lowering blood lipids, antioxidant effects, and anti-tumor properties. With the deepening research into the components of goji berries and the increasing awareness of health preservation, the demand for goji berries has surged rapidly. Consequently, the cultivation area for goji berries has been expanding gradually. In 2023, China's goji berry cultivation covered an area of 1.83 million mu (approximately 274,500 acres), with a fresh fruit yield of 1.4 million tons.

Plant leaves play a pivotal role in defending against both biotic and abiotic stressors. A significant correlation exists between leaf thickening and the enhancement of resistance [4]. The anatomical structure of leaves is intricately linked to the stress tolerance of plants. When subjected to external environmental stresses, plants undergo numerous morphological, physiological, biochemical, and anatomical changes [5,6]. The anatomical characteristics indicate that plants with thinner leaf thicknesses, cuticles, palisade tissues, and spongy tissues exhibit reduced resistance. In investigations involving *Canarium album* (Lour.) varieties and *Lactuca sativa* var Hort., drought stress was observed to result in increased thickness of the upper epidermis and palisade mesophyll, elevated stoma density, and decreased stoma closure [7,8]. The thickness of the cuticle, stoma density, looseness of palisade and leaf tissues, as well as the thickness of the lower epidermis and spongy tissue, along with the ratio of palisade to spongy tissue and other indicators such as leaf tissue density and overall leaf thickness have minimal impact on the drought resistance of leaves [9]. Conversely, studies on the anatomical structures of *Michelia figo* (Lour.) Spreng reveal that thicker palisade tissue correlates with enhanced cold resistance; additionally, a greater ratio of palisade to spongy tissue is associated with stronger cold tolerance [10]. Walnut varieties exhibiting superior cold resistance possess thicker palisade and spongy tissues, along with a higher palisade/spongy tissue ratio compared to those demonstrating poorer cold resilience [11]. Furthermore, an evaluation of peach germplasm resources indicates a direct positive correlation between leaf thickness and cold resistance [12].

This study selected 36 different cultivars (lines) of goji to evaluate the resilience of these goji germplasm resources and the relationship between different leaf anatomical structure indicators and various resilience levels, using paraffin sectioning, frozen sectioning, the membership function method, principal component analysis, clustering heatmaps, and hierarchical clustering. Additionally, a comprehensive resilience ranking of the goji cultivars was conducted, the significant relationships between different indicators and resistances were assessed, and 36 goji cultivars (lines) were classified based on similarity. The following issues will be initially clarified: (1) What are the characteristics of the leaf anatomical structures of the 36 germplasm resources of different goji, and what is the relationship between each indicator and goji resistance? (2) Are there differences in resilience regarding leaf anatomical structure among the 36 selected healthy goji plants? This experiment will help explain how the leaf structure of goji berries adapts to different stresses and provide a preliminary assessment of the resilience of goji cultivars (lines). The aim is to offer a reference for the identification and evaluation of goji cultivars (lines), thereby accelerating the selection and breeding process for superior goji varieties.

2. Materials and Methods

2.1. Materials

The goji resources utilized in the experiment originated from the Luhuatai goji Germplasm Resource Garden, goji Research Institute of Ningxia Academy of Agriculture and Forestry (38°64′ N, 106°15′ E), following standard production and management protocols. Sampling of the 36 different cultivars (lines) of goji was undertaken on a beautiful morning in April 2024. Robust goji plants exhibiting optimal growth were chosen, and leaves from the fourth position downward were harvested, with three plants picked for each goji resource. The 36 different cultivars (lines) of goji for the examination are presented in Table 1.

Table 1. The 36 cultivars (lines) of goji examined in this study.

Abbreviation	Cultivar (Line)	Abbreviation	Cultivar (Line)
NC1	*L. barbarum* 'Ningqicai 1'	He3	*L. barbarum* 'He 3'
NC3	*L. barbarum* 'Ningqicai 3'	7-8	*L. barbarum* '7-8'
NC4	*L. barbarum* 'Ningqicai 4'	2-182	*L. barbarum* '2-182'
NC5	*L. barbarum* 'Ningqicai 5'	2-184	*L. barbarum* '2-184'
NC6	*L. barbarum* 'Ningqicai 6'	LR	*L. ruthenicum* Murr.
NC7	*L. barbarum* 'Ningqicai 7'	LC	*L. Chinense* Mill
NC8	*L. barbarum* 'Ningqicai 8'	LCy	*L. cylindricum* Kuang
NC9	*L. barbarum* 'Ningqicai 9'	LY	*L. yunnanense* Kuang
NC10	*L. barbarum* 'Ningqicai 10'	Guangdong	*L. chinense* 'Guangdong'
1818	*L. barbarum* '1818'	Amercicanum	*L.* americanum Jacp
1821	*L. barbarum* '1821'	LezhiB	*L. dasystemum* Pojark 'LezhiB'
1825	*L. barbarum* '1825'	Lezhi	*L. dasystemum* 'Lezhi'
N1	*L. barbarum* 'Ningqi 1'	14-01	*L. barbarum* '14-01'
N5	*L. barbarum* 'Ningqi 5'	1-173	*L. barbarum* '1-173'
N7	*L. barbarum* 'Ningqi 7'	1-368	*L. barbarum* '1-368'
N10	*L. barbarum* 'Ningqi 10'	Tianjing 3	*L. barbarum* 'Tianjing 3'
Z99	*L. barbarum* 'Z99'	4-1	*L. barbarum* '4-1'
Z77	*L. barbarum* 'Z77'	6082	*L. barbarum* '6082'

2.2. Methods

2.2.1. Examination of the Stomata on the Abaxial Epidermis of Goji Leaves

Three plants were selected per barbary wolfberry, and the leaves of the fourth leaf were taken from the bud down. Slides were prepared using the nail polish imprint technique. The lower epidermis of goji leaves was coated with a coat of colorless nail polish. The lower epidermis' nail paint was carefully pulled off with tweezers once it had dried, and it was then put on a glass slide. Under a microscope, the slides were examined and photographed, and measurements of stomatal length, stomatal breadth, stomatal apparatus length, stomatal apparatus width, stomatal density, and stomatal aperture were made in addition to noting the number of stomata. The number of stomatal apparatuses per field of vision was used to compute stomatal density, and the ratio of stomatal width to stomatal length was used to calculate stomatal aperture. Observations were conducted using the PA53 FS6 Intermediate biological fluorescence microscope by Motic China Group Co., Ltd. (Xiamen, China). From each slide, three distinct and clear areas were chosen for analysis. Images and measurements were captured using the Motic Images Plus 3.1 (×64) software. The relevant metrics were recorded for each area, and the mean values were then used as the data for the respective leaf parameters [13].

2.2.2. Sampling and Section Making

Three plants exhibiting uniform and vigorous development were chosen for each goji resource. One tender leaf was extracted from the fourth leaf position downward from the terminal bud of each plant. Tissue blocks measuring 5 mm × 5 mm were excised from both sides of the leaf vein and subsequently immersed in 50% FAA fixative for over 72 h at roughly 4 °C for fixation prior to future utilization.

Leaf cross-sectional tissue sections were prepared via the paraffin sectioning technique. Three leaves of each variety goji were used to make sections [14]. The main processes involved ethanol dehydration, followed by embedding in xylene transparent paraffin, spreading and patching with a Shanghai Junjie Electronics Co., Ltd. (Shanghai, China) microtome to form solid green dye tablets, which were placed on Canadian neutral gum seal sheet and made into permanent slices for subsequent observation.

Frozen Sections: Three plants exhibiting uniform and vigorous development were chosen for each goji resource. One tender leaf was extracted from the fourth leaf position downward from the terminal bud of each plant. Tissue blocks of 5 mm × 5 mm were excised from both sides of the leaf vein and deposited in a 10 mL centrifuge tube, which was thereafter stored at −80 °C in a freezer. Wax sections were made with the oil red staining technique, which primarily involves OCT embedding, cryostat sectioning, oil red staining, and mounting with neutral balsam to produce permanent glass slides for future inspection. The portions were examined.

To observe and take pictures of tissue sections, the sections must be placed under a microscope. Multiple tissue sections from the identical strain exhibiting distinct and intact staining structures were chosen for examination. Seven indicators were assessed: thickness of the upper cuticle (TUC), thickness of the lower cuticle (TLC), thickness of the upper epidermis (TU), thickness of the lower epidermis (TL), thickness of the palisade tissue (TP), thickness of the spongy tissue (TS), and total leaf thickness (LT). Each tissue strip was examined and photographed in three fields of view, with three tissue strips analyzed for each substance. The mean values were utilized as the indication values. Frozen section observation involves first placing the frozen sections under a microscope for photography, selecting three replicates, and then using ImageJ (1.6.0_24) for batch analysis of the frozen paraffin sections [15]. The parts stained red represent the cuticle of the leaf. The area of the parts stained red is measured as a proportion of the entire section's area.

2.2.3. Analysis of Field Infection Experiments

An investigation of field *A. pallida* on goji was performed in accordance with the local norm "DB64/T852-2013" [16]. The 5-point sample technique was employed, with 2 plants randomly chosen at each location. From each plant, one branch was randomly selected from each of the five orientations: east, west, south, north, and center. The extent of mite damage was evaluated on 25 leaves at the apex of each branch in accordance with the mite damage classification criteria. The mite infestation index was then computed.

2.3. Data Processing

The data from the observable indicators were systematically grouped and initially computed using Excel software. The subsequent ratios and indices were calculated: palisade tissue thickness/spongy tissue thickness (P/S), spongy tissue thickness/total leaf thickness (S/L), upper epidermis thickness/spongy tissue thickness (U/S), palisade tissue thickness/total leaf thickness (P/L), leaf tissue compactness ratio (CTR), leaf tissue looseness ratio (SR), and plasticity index (PI). The equations are as follows: P/S = thickness of palisade tissue/thickness of spongy tissue; P/L is calculated as the thickness of palisade tissue divided by the thickness of the leaf. S/L = spongy tissue thickness/leaf thickness; CTR = (palisade tissue thickness/leaf thickness) × 100%; SR = (spongy tissue thickness/leaf thickness) × 100% [17]. PI was computed using Equation (1); CV was determined using Equation (2).

The resistance of each goji strain is determined using the membership function approach. The particular algorithm is presented in Equation (3). If a specific indicator exhibits a negative correlation with its resistance, the inverse membership function is employed for conversion. The calculating procedure is delineated in Equation (4) [17], wherein Xi represents the fixed value of each indicator, and X_{min} and X_{max} denote the minimum and maximum values of a specific indicator of the leaf anatomical structure across all populations. The average membership function values of the markers pertaining to resistance in the leaf anatomical structure of each strain are computed. The magnitude of these values exhibits a positive correlation with the stress resistance of goji.

$$PI = (Max - Min)/Max \quad (1)$$

$$CV = Standard\ deviation/average \times 100\% \quad (2)$$

$$R(Xi) = (Xi - Xi_{min})/(Xi_{max} - Xi_{min}) \quad (3)$$

$$R(Xi) = 1 - (Xi - Xi_{min})/(Xi_{max} - Xi_{min}) \quad (4)$$

where i is 1, 2, 3, . . ., 36.

Principal Component Analysis Method: Normalized and descriptive analysis of the organized data using Origin 2024 and SPSS 27 software, followed by principal component analysis to rank the resistance of different goji berry varieties.

Hierarchical Clustering: Clustering is conducted on the data using SPSS to analyze the relationships between different goji berry varieties. Origin 2024 is used to generate a heat map showing the correlation and the relationship between various indices and resistance.

ImageJ was utilized for the batch analysis of frozen paraffin sections to determine the wax ratio, Oil red staining renders the leaf cuticle wax layer red, and the proportion of the red area to the total area of the section is calculated using ImageJ, defined as the area of the wax layer divided by the total area of the leaf section. The Phantom 9900XL scanner facilitated the scanning of leaves from the field infestation experiment involving mites. Subsequently, the Vincent Plant Leaf Multi-functional Analyzer (Hangzhou Wanshen Testing Technology Co., Ltd., Hangzhou, China) was employed to analyze the scanned leaf data, which encompassed the number of leaves, total leaf area, total gall area, and the number of galls. The infestation area ratio and the average number of galls were subsequently calculated. Infestation area ratio is calculated by dividing the total gall area by the total leaf area. The average number of galls is determined by dividing the number of galls by the number of leaves. The larger the proportion of infected area and the average number of galls, the weaker the resistance of the goji variety to gall mites.

3. Results Analysis

3.1. Analysis of Leaf Structural Characteristics of the 36 Tested Cultivars (Lines) of Goji

3.1.1. Differences in Leaf Anatomical Structure

As can be seen from the slice map (Figure 1), there are obvious ridges in the dorsoventral surface of different barbary wolfberry leaves and an obvious cuticle outside the cells of the epidermis. The obviously differentiated palisade tissue and spongy tissue show the barbary wolfberry leaves. The distinct palisade and spongy tissues in goji leaves indicate a dorsiventral leaf structure. The observation results show that the palisade tissue in Z99, N10, LC, LCy, Guangdong, 1-173, and 6082 consists of one to two layers, while in NC5, 1825, N1, N5, N7, He3, 2-182, LR, LY, 14-01, 1-368, and 4-1, it consists of two to three layers. For most goji species, the palisade tissue is composed of a single layer of well-arranged columnar cells.

To investigate the variations in anatomical traits among different cultivars (lines), an analysis of the data concerning the anatomical structure of leaves from these goji plants was performed. The findings revealed the maximum leaf thickness measured in LR, while the minimum thickness was recorded in 6082. Regarding epidermal tissue, with the exception of leaves from 1821, 1825, LezhiB, Tianjing 3, and 4-1, it was noted that the thickness of the upper cuticle surpassed that of the lower cuticle. The thickness of the upper epidermis in LR was the highest, followed closely by that of LezhiB. In contrast, the upper epidermis of NC4 exhibited the thinnest measurement. The lower epidermis thickness of LR also ranked as the greatest, followed by N7, while NC9 had the thinnest lower epidermis among these samples. In mesophyll tissue comparing palisade and spongy tissue thickness, the palisade tissue in LR exhibited the greatest thickness, whereas that of NC5 displayed the smallest thickness. Similarly, in the spongy tissue, LR showed the highest thickness, while 6082 had the lowest. Concerning leaf tissue compactness and porosity, both metrics for LCy were maximal. The analysis of plasticity indices revealed minimal variation in the plasticity range among the various anatomical structures of the 36 goji germplasm resources, with values ranging from 0.63 to 0.86 (Supplementary Table S1).

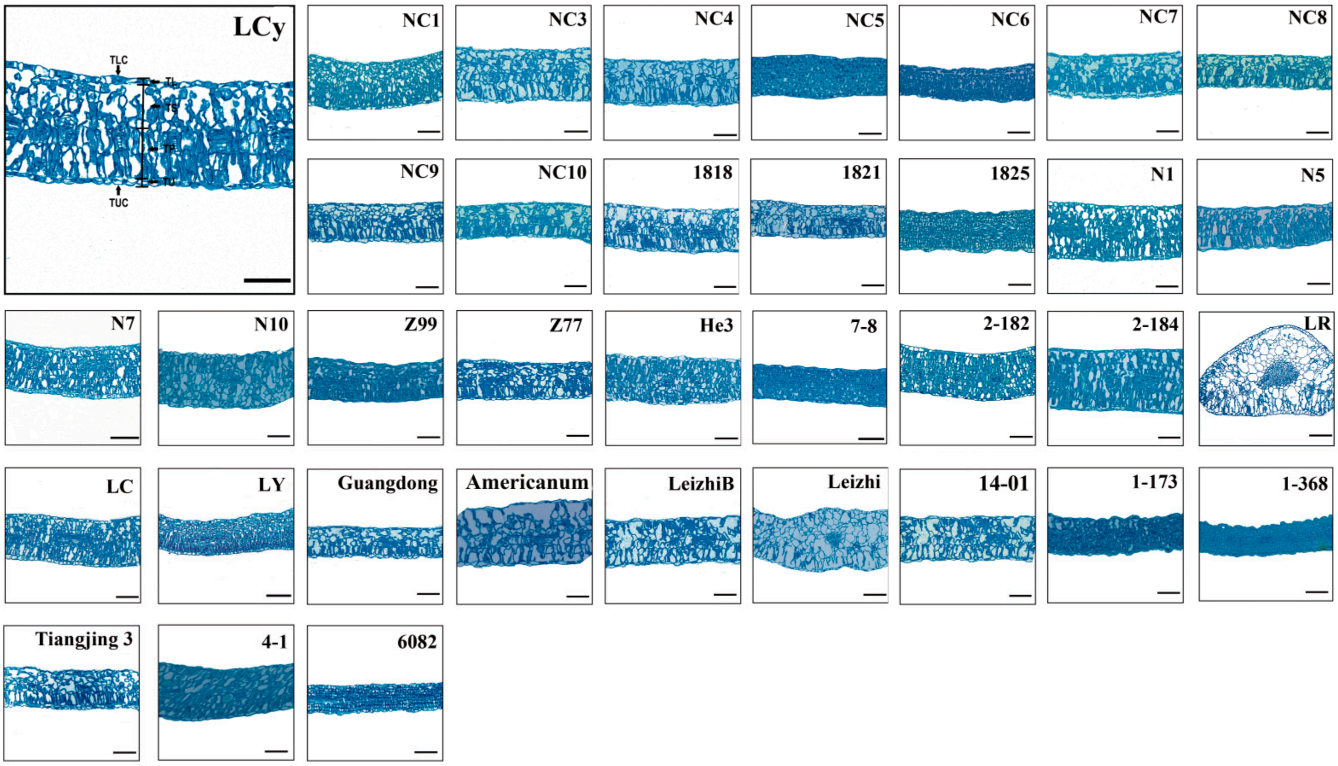

Figure 1. Anatomical structures of leaf blades in the 36 tested cultivars (lines) of goji. TU, Thickness of upper epidermis; TL, Thickness of lower epidermis; TP, Thickness of palisade tissue; TS, Thickness of spongy tissue; TUC, Thickness of the upper cuticle; TLC, Thickness of the lower cuticle. The image numbers correspond to the goji varieties listed in Table 1. The sections were stained with Safranin and Fast Green, where the cellulose cell walls and sieve tubes appear blue. Bar = 100 µm.

3.1.2. Comparative Analysis of Leaf Stomatal Characteristics

Leaf stomata function as natural conduits for insect herbivory on plants. An elevated density of leaf stomata augments the suitability for insect feeding; contrarily, a reduced density mitigates this suitability. Furthermore, plants demonstrating enhanced drought resistance typically possess smaller and denser stomata. The motility of stomata constitutes one of the pivotal factors for maintaining the osmotic potential of plant cells, and the structural attributes of stomata are intimately associated with the drought resistance of plants [18]. Since most plants have a greater number of stomata on the lower epidermis of their leaves than on the upper epidermis, observations and analyses of the stomata on the lower epidermis of different goji leaves indicate this trend (Figure 2). The stomata length across all germplasm resources ranged from 17.76 to 59.60 µm, exhibiting a coefficient of variation of 21%. Among these, in terms of stomatal length, Americanum goji berry exhibited the greatest dimension, whereas Z77 displayed the shortest, with a statistically significant difference observed between these two extremes. The width of the stomata ranged from 2.68 to 16.79 µm, exhibiting a coefficient of variation of 28%. Notably, Tianjing 3 displayed the largest stomata width, while NC6 exhibited the smallest; the difference between the two was significant. The stomata openness varied between 0.5 and 0.81, with a coefficient of variation of 38%. Among the cultivars, 1825 demonstrated the greatest stomata openness, whereas *LR* showed the least; again, this difference was statistically significant. The stomata density of 1825 and N10 was significantly different from that of NC7, 1818, He3, and 1-173. Additionally, the length of the stomata organ ranged from

21.55 to 88.67 μm, with a coefficient of variation of 18%. Notably, Americanum goji berry had the longest stoma organ length, while N5 exhibited the shortest; this difference was statistically significant. The width of the stoma organ spanned from 16.97 to 52.37 μm, with a coefficient of variation amounting to 18% (Supplementary Table S2). Significantly, Americanum goji berry manifested the maximal width of the stoma organ, while Z77 had the narrowest, with a statistically significant difference. These results indicate significant variations exist in stoma length, width, density, and the ratio of stoma length to width among goji germplasm resources.

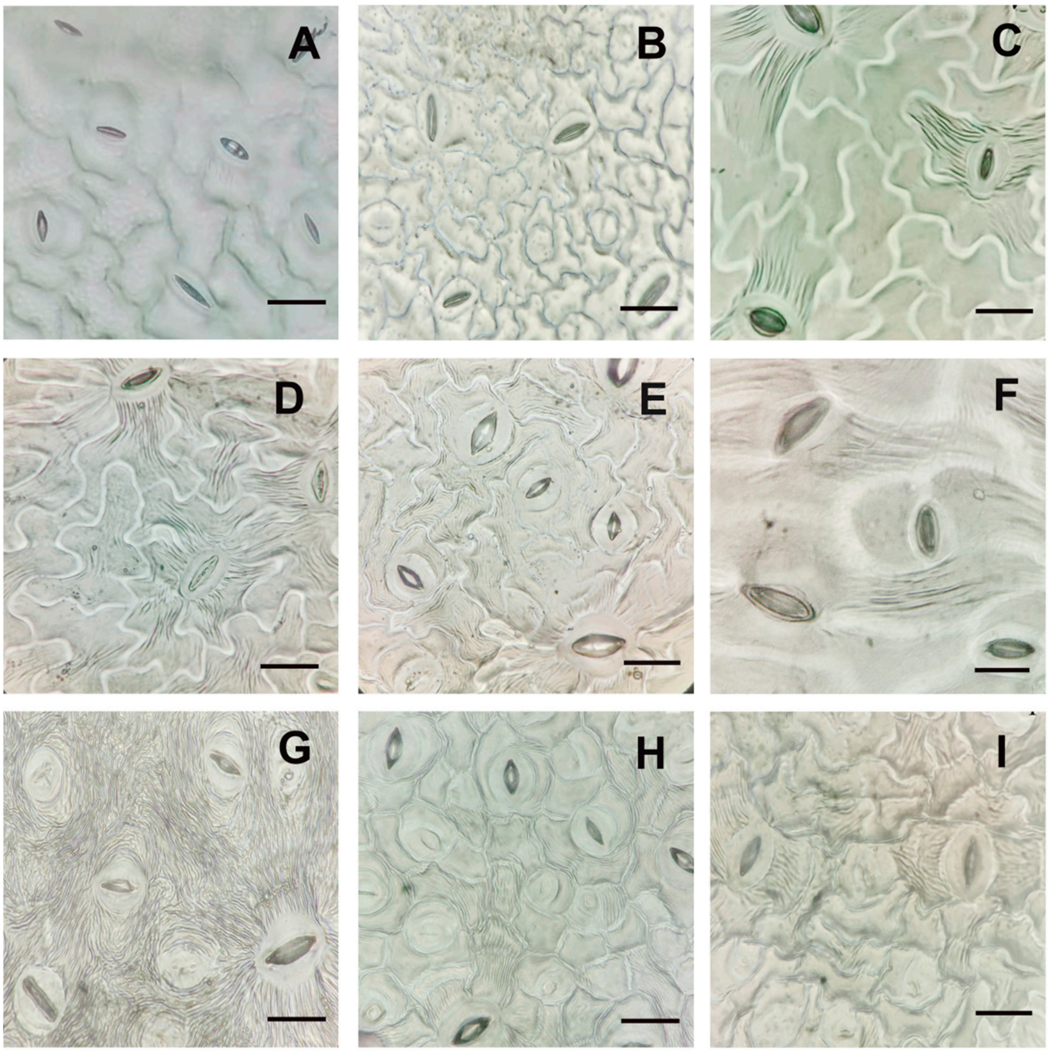

Figure 2. Stomata in the lower epidermis of the leaves of different cultivars (lines). (**A**) Americanum; (**B**) Z77; (**C**) Tianjing 3; (**D**) NC6; (**E**) 1825; (**F**) LR; (**G**) N10; (**H**) NC7; (**I**) N5. Bar = 100 μm.

3.1.3. Frozen Section Staining Indicates the Proportion of Wax Content

The resistance or sensitivity of plants to pathogens or insects is closely related to the accumulation and composition of wax on their leaves. Plants with higher wax content are more resistant to insects. According to the analysis of the proportion of wax in leaves of 36 different cultivars (lines) of goji germplasm resources (Figures 3 and 4), the proportion of wax in the leaves of these resources varied. LR, LCy, and Tianjing 3 had the top three wax contents, suggesting that they may have better resistance than other cultivars (lines). In contrast, the wax content of NC10, Guangdong, and Lezhi was relatively low.

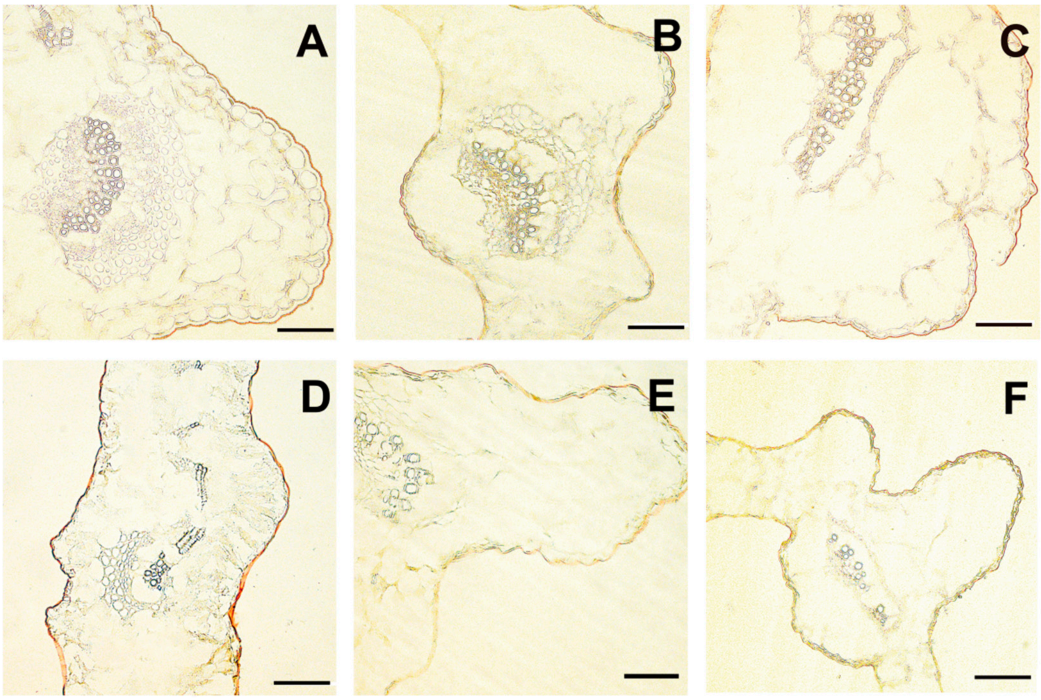

Figure 3. Part of goji leaf wax frozen section. (**A**) LR; (**B**) LCy, (**C**) Tianjing 3; (**D**) Lezhi; (**E**) Guangdong; (**F**) NC10. The sections stained with the Oil Red method show the wax layer as the part that turned red in the image. Bar = 100 μm.

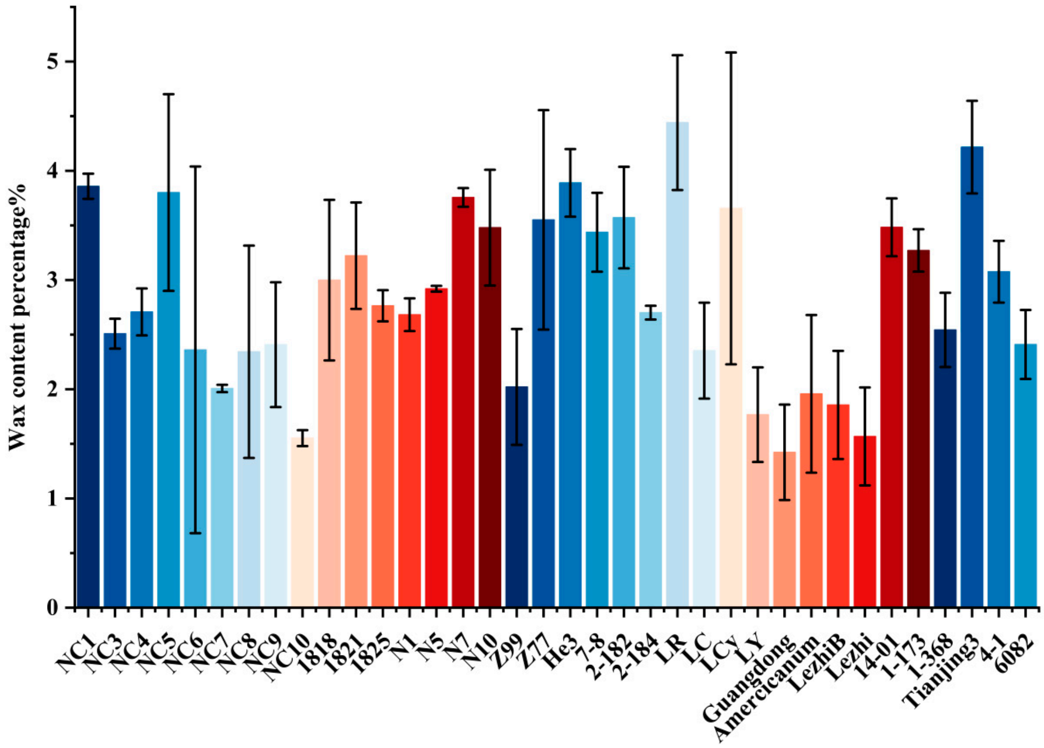

Figure 4. Wax proportion in frozen sections of the 36 different goji cultivars (lines) tested. The error bars represent the difference between the wax proportion of individual goji lines and the mean wax proportion of the same line; the goji cultivars (lines) are represented by the abbreviations in the image, as listed in Table 1.

3.1.4. Correlation Analysis of Anatomical Indices from Leaf Samples Among Goji Cultivar (Line) Germplasm Resources

Through the correlation analysis of the proportion of different wolfberry parts (Figure 5), it was found that TU (thickness of upper epidermis) had a highly significant positive correlation with TL, TP, TS, TUC, TLC and LT (leaf thickness) ($p \leq 0.01$); TL had a highly significant positive correlation with TP, TS, TLC and LT($p \leq 0.01$), and a significant positive correlation with TLC ($p \leq 0.05$); TP had a highly significant positive correlation with TS, LT and P/L (Palisade tissue and leaf ratio) ($p \leq 0.01$) and a significant positive correlation with TLC, P/S ($p \leq 0.05$); TS had a highly significant positive correlation with TUC, TLC, LT and S/L ($p \leq 0.01$), and a highly significant negative correlation with U/S ($p \leq 0.01$). TUC showed a highly significant positive correlation with TLC, LT($p \leq 0.01$); TLC had a highly significant positive correlation with LT ($p \leq 0.01$); LT showed a highly significant negative correlation with U/S ($p \leq 0.01$); P/S (Palisade tissue and spongy tissue ratio) exhibited a highly significant positive correlation with P/L ($p \leq 0.01$), a significant positive correlation with U/S ($p \leq 0.05$), and a highly significant negative correlation with S/L ($p \leq 0.01$); the P/L ratio had a highly significant negative correlation with S/L ($p \leq 0.01$); the S/L ratio showed a highly significant negative correlation with the U/S ratio ($p \leq 0.01$). Multiple correlations among other traits were detected, but they did not reach statistical significance.

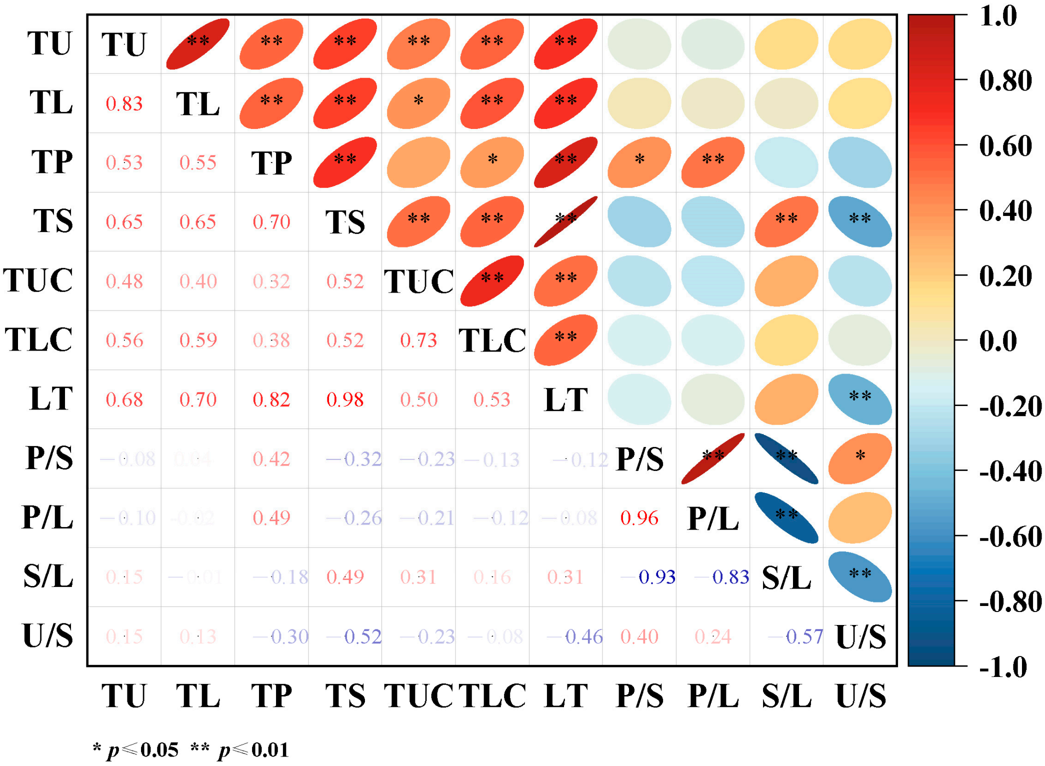

Figure 5. Correlation analysis of leaf character traits. Red denotes a positive correlation between traits, whereas blue signifies a negative correlation. The intensity of the color indicates the strength of the correlation between traits, with darker shades representing a stronger relationship. The numbers in the graph indicate the degree of correlation, with higher numbers suggesting a stronger correlation. * $p \leq 0.05$ indicates a statistically significant correlation between traits, and ** $p \leq 0.01$ indicates a highly statistically significant correlation. Definitions of traits: TU: Thickness of upper epidermis; TL: Thickness of lower epidermis; TP: Thickness of palisade tissue; TS: Thickness of spongy tissue; TUC: Cuticle thickness of upper epidermis; TLC: Thickness of lower epidermis cell; LT: Leaf thickness; P/S: Palisade tissue and spongy tissue ratio; P/L: Palisade tissue and leaf ratio; S/L: Spongy tissue and leaf ratio; U/S: Upper epidermis and spongy tissue ratio.

3.2. Comprehensive Analysis and Evaluation of Resistance of Goji Cultivars (Lines)

3.2.1. The Subordinate Function Approach for Assessing the Stress Resistance of Goji Cultivars (Lines)

Utilizing the membership function method, the pest resistance of 36 cultivars (lines) of goji was evaluated based on six criteria: TU, TP, TUC, TLC, P/L, and LT [19]. For assessing drought resistance, the following six indicators were selected: TU, TP, TUC, TLC, P/S, LT [20]. Since a plant's cold resistance is closely related to the palisade to spongy ratio, the same set of six criteria—TU, TP, TS, TLC, P/L, and LT—were used as the evaluation metrics for cold resistance [21]. After computing these indicators through the membership function and weighted average score, it was ascertained that among the 36 cultivars (lines) of goji under investigation, LR manifested superior cold and drought resistance, while LCy displayed optimal insect resistance (Table 2).

Table 2. The stress resistance of 36 cultivars (lines) of goji resources was scored using the membership function technique. The resistance of goji berries to adversity is assessed by selecting different indicators using the membership function method. A higher score implies greater resilience. For positive indicators, the membership function is $R(Xi) = (Xi - Xi_{min})/(Xi_{max} - Xi_{min})$. For negative indicators, the membership function is $R(Xi) = 1 - (Xi - Xi_{min})/(Xi_{max} - Xi_{min})$.

Cultivar (Line)	Insect Resistance Score	Order	Drought Resistance Score	Order	Cold Resistance Score	Order	Total Resistance Score	Order
NC1	0.35	15	0.37	11	0.34	13	0.35	13
NC3	0.19	28	0.22	23	0.21	24	0.21	24
NC4	0.3	20	0.26	19	0.28	18	0.28	18
NC5	0.12	33	0.16	27	0.12	28	0.13	28
NC6	0.19	28	0.19	24	0.18	25	0.19	25
NC7	0.17	30	0.17	26	0.15	27	0.16	27
NC8	0.28	21	0.27	18	0.27	19	0.27	19
NC9	0.3	20	0.32	14	0.29	17	0.3	17
NC10	0.18	29	0.17	26	0.17	26	0.17	26
1818	0.31	18	0.29	17	0.31	15	0.3	17
1821	0.42	9	0.4	8	0.41	8	0.41	8
1825	0.24	24	0.24	21	0.23	22	0.24	21
N1	0.26	23	0.29	17	0.25	21	0.27	19
N5	0.61	3	0.5	3	0.64	2	0.58	3
N7	0.5	5	0.49	4	0.49	5	0.49	5
N10	0.37	13	0.36	12	0.35	12	0.36	12
Z99	0.21	26	0.25	20	0.21	24	0.22	23
Z77	0.31	19	0.3	16	0.3	16	0.3	17
HE3	0.43	8	0.37	10	0.41	8	0.4	9
7-8	0.36	14	0.31	15	0.36	11	0.34	14
2-182	0.41	10	0.34	13	0.4	9	0.38	11
2-184	0.33	17	0.29	17	0.31	15	0.31	16
LR	0.69	2	0.72	1	0.68	1	0.7	1
LC	0.46	7	0.38	9	0.45	7	0.43	7
LCy	0.72	1	0.57	2	0.57	3	0.62	2
LY	0.3	20	0.22	23	0.32	14	0.28	18
Guangdong	0.16	32	0.17	26	0.15	27	0.16	27
Americanum	0.27	22	0.25	20	0.26	20	0.26	20
LezhiB	0.38	12	0.42	7	0.38	10	0.39	10
Lezhi	0.49	6	0.48	5	0.47	6	0.48	6
14-01	0.51	4	0.47	6	0.5	4	0.5	4
1-173	0.2	27	0.18	25	0.18	25	0.19	25
1-368	0.23	25	0.23	22	0.22	23	0.23	22
Tianjing 3	0.39	11	0.36	12	0.38	10	0.38	11
4-1	0.34	16	0.34	13	0.32	14	0.33	15
6082	0.16	31	0.16	28	0.17	26	0.16	27

3.2.2. Evaluating the Influence of Various Indicators on the Stress Resistance of Goji Cultivars (Lines) Using Principal Component Analysis

Principal component analysis (PCA) was adopted to categorize and streamline the diverse resistance-corresponding indicators of the 36 tested goji cultivars (lines), with two principal components being extracted from each type. Among the three principal components, the factor loadings corresponding to each indicator of the 36 cultivars (lines) demonstrated marked heterogeneity. The correlation coefficients (load matrix) between the principal components and other indicators reflected the relative magnitude and orientation of the principal component loadings of certain indicators. The greater the absolute value of the correlation coefficient, the closer the association and the more substantial the contribution to the principal component.

From Tables 3 and 4, it is evident that for the analysis of insect resistance in goji, the cumulative contribution of the first two principal components amounted to 82.44%. Notably, the absolute values of the relative coefficient loadings for LT and TS in the first principal component and P/L in the second principal component were significant, indicating their capacity to more effectively represent the insect resistance across various goji cultivars (lines). Consequently, LT, TS, and P/L emerged as pivotal indicators for a more precise evaluation of the insect resistance characteristics of goji cultivars (lines).

Table 3. The characteristic values and contribution rates associated with the principal components for various stress resistances are presented. The principal components are derived from the extracted characteristic values, adhering to a criterion where the cumulative contribution rate exceeds 70%.

	Principal Component	**Eigen Value**	**Contribution/%**	**Cumulative Contribution/%**
Insect resistance	I	3.58	59.71	59.71
	II	1.36	22.74	82.44
Drought resistance	I	3.22	53.73	53.73
	II	1.45	24.18	77.91
Cold resistance	I	3.23	53.77	53.77
	II	1.41	23.42	77.18

Table 4. The principal component analysis of each factor loading matrices. TU: Thickness of upper epidermis; TP: Thickness of palisade tissue; TS: thickness of the spongy tissue; TUC: Cuticle thickness of upper epidermis; TLC: Thickness of lower epidermis cell; P/S: Palisade tissue and spongy tissue ratio; P/L: Palisade tissue and leaf ratio; The larger the absolute value of the loadings matrix coefficient, the closer the relationship and the greater the contribution to the principal component.

Insect resistance	Principal component	TU	TP	TS	TLC	LT	P/L
	I	0.81	0.82	0.93	0.68	0.97	−0.03
	II	−0.13	0.55	−0.19	−0.22	0.00	0.98
Drought resistance	Principal component	TU	TP	LT	TUC	TLC	P/L
	I	0.81	0.76	0.89	0.75	0.79	−0.01
	II	−0.06	0.62	0.11	−0.38	−0.29	0.91
Cold resistance	Principal component	TU	TP	LT	P/S	TUC TLC	
	I	0.81	0.75	0.89	−0.06	0.75	0.80
	II	−0.01	0.61	0.12	0.90	−0.38	−0.27

In the analysis of drought resistance, the combined contribution of the first two principal components reached 77.91%. When evaluating the drought resistance of various goji germplasm resources, we utilized the indices TU and LT from the first principal component, as well as P/L from the second principal component. As a result, the indices TU, LT, and P/L were identified as key factors in assessing the drought resilience of goji genetic resources.

The first two components collectively accounted for 77.18% of the assessed cold resistance. The TU, LT, and TLC indicators from the first primary component, along with P/S from the second principle component, were utilized to assess the cold resistance of different goji cultivar (line) germplasm resources. Thus, TU, LT, TLC, and P/S functioned as more dependable indicators for evaluating the cold hardiness of goji cultivars (lines). After normalizing anatomical indicator data for goji germplasm and conducting principal component analysis to ascertain their overall stress resistance scores, the findings shown in Table 5 revealed that LR, LCy, and N7 exhibited the highest levels of comprehensive stress resistance. In contrast, NC7, Guangdong, and Z99 were recognized as the varieties exhibiting the least resistance. The results of this analysis align closely with the findings from the membership function technique, indicating that LR and N7 have enhanced overall stress resistance capacities. A correlation analysis between the structures of principal component analysis and the membership function method indicated a substantial relationship between the two.

Table 5. The stress resistance of goji by principal component analysis, wherein principal components are derived based on extracted characteristic values, adhering to a requirement of a cumulative contribution rate exceeding 80%. Principal component score = coefficient matrix of linear combinations × standardized data, where the coefficient of linear combinations is the loading coefficient divided by the square root of the appropriate eigenvalue.

Cultivar (Line)	Score	Order	Cultivar (Line)	Score	Order
LR	275.34	1	LY	34.66	19
N7	158.51	2	6082	33.29	20
LCy	142.56	3	2-184	27.45	21
N5	132.30	4	1818	26.35	22
LezhiB	131.12	5	NC9	25.19	23
14-01	122.01	6	1825	23.87	24
Lezhi	118.64	7	NC8	9.71	25
1821	92.95	8	NC4	6.99	26
Tianjing 3	71.12	9	Americanum	5.19	27
N10	70.21	10	N1	2.09	28
NC1	55.89	11	NC6	−0.52	29
LC	54.75	12	1-368	−1.45	30
7-8	54.28	13	NC5	−8.56	31
2-182	52.78	14	1-173	−10.86	32
NC3	50.12	15	NC10	−12.34	33
He3	45.73	16	Z99	−12.99	34
4-1	44.69	17	Guangdong	−25.69	35
Z77	41.00	18	NC7	−36.39	36

3.2.3. Cluster Heat Map Analysis

To conduct a direct examination of the variances in diverse indices and resistance modalities, a heatmap was utilized to visualize the modifications in goji traits under multifarious stress circumstances, with clustering serving to reflect the correlations between disparate goji germplasm resources and their corresponding indices. The findings indicate varying correlations between insect resistance and the six indicators: TU, TP, TS, LT, TLC, and P/L (Figure 6A). LR exhibited enhanced insect resistance due to the influence of TU, TP, TS, LT, and TLC. In LCy, P/L exerted a significant influence. For LezhiB, TU significantly influenced its insect resistance. TUC and P/L exerted a comparatively significant influence on the evaluated goji germplasm resources.

Figure 6B demonstrates that the cold resistance of goji cultivars (lines) exhibited varying correlations with the six indicators: TU, TP, TUC, TLC, P/S, and LT. For TU, TP, TUC, and TLC, P/S significantly influenced cold resistance. In N5, cold resistance was predominantly affected by P/S. In LCy, P/S served as the primary indicator influencing cold resistance. For LezhiB, TU significantly enhanced cold resistance. TUC and TLC significantly influenced the cold resistance of goji germplasm resources.

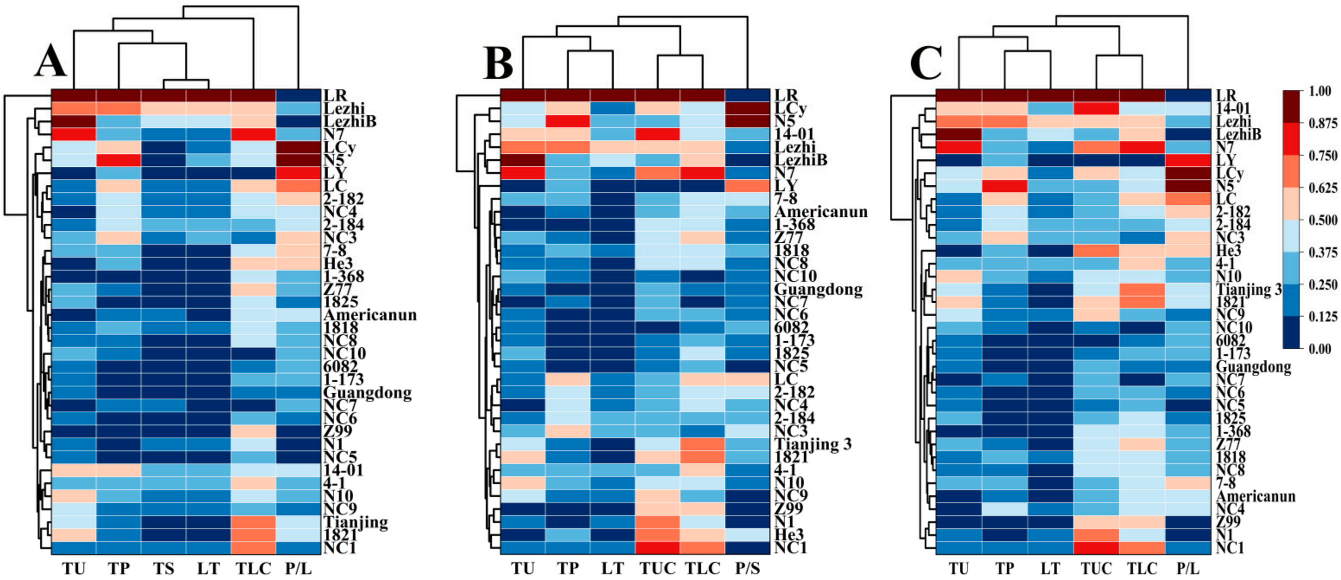

Figure 6. Clustering analysis of different cultivars (lines) of goji traits and associated stress resistance, presented as a heatmap. (**A**) illustrates the heatmap clustering analysis of various goji traits and insect resistance; a color closer to red indicates a stronger correlation between the trait and the goji line. (**B**) illustrates the heatmap clustering analysis of various goji traits in relation to cold resistance. (**C**) illustrates the heatmap clustering analysis of various goji traits in relation to drought resistance. TU refers to the thickness of the upper epidermal cells; TP denotes the thickness of the palisade tissue; TUC indicates the thickness of the upper epidermal cuticle; TLC represents the thickness of the lower epidermal cuticle. P/S refers to the palisade-to-spongy ratio, while P/L denotes the palisade-to-leaf ratio. CTR refers to the compactness of leaf tissue, while SR denotes the sponginess of leaf tissue. The numerical identifiers for the 36 goji cultivars (lines) depicted in the figure correspond to the goji entries presented in Table 1.

Figure 6C demonstrates that the six indicators TU, TP, TUC, TLC, LT, and P/L had differing impacts on the drought resistance of goji resources. The drought resistance of LR was primarily influenced by TU, TP, TUC, TLC, and LT. In LCy, P/L was identified as the primary influencing factor. For N5, P/L was identified as the primary indicator of its drought resistance. For *L. dasystemum* 'LezhiB', the TU index had a more significant impact on drought resistance. In conclusion, for the 36 tested goji cultivars (lines), TUC and TLC were significant indicators influencing drought resistance.

3.3. Comprehensive Cluster Analysis of 36 Different Cultivars (Lines) of Goji Germplasm Resources

A cluster analysis was conducted to examine the relationships among goji cultivars (lines) based on the average values of anatomical structure indicators of goji leaves. Indicators of organizational structure were classified through the application of Euclidean distance. The findings indicated that at a distance value of 5.0, the 36 materials were categorized into four clusters. Cluster I included 24 goji cultivars (lines); Cluster II comprised 9 goji cultivars (lines); Cluster III contained two goji cultivars (lines), both from the Lezhi cultivars (lines), exhibiting similar resistance traits; Cluster IV consisted of a single goji cultivar (lines), LR, which was assessed as having the highest overall resistance (Figure 7). The cluster analysis revealed a significant similarity among the goji resources within each of the four clusters, indicating that the resources in each cluster are more closely related to one another. The observed similarity among the goji cultivars (lines) across the four clusters was minimal, indicating that the clustering of various goji cultivars (lines) correlates with their resistance characteristics.

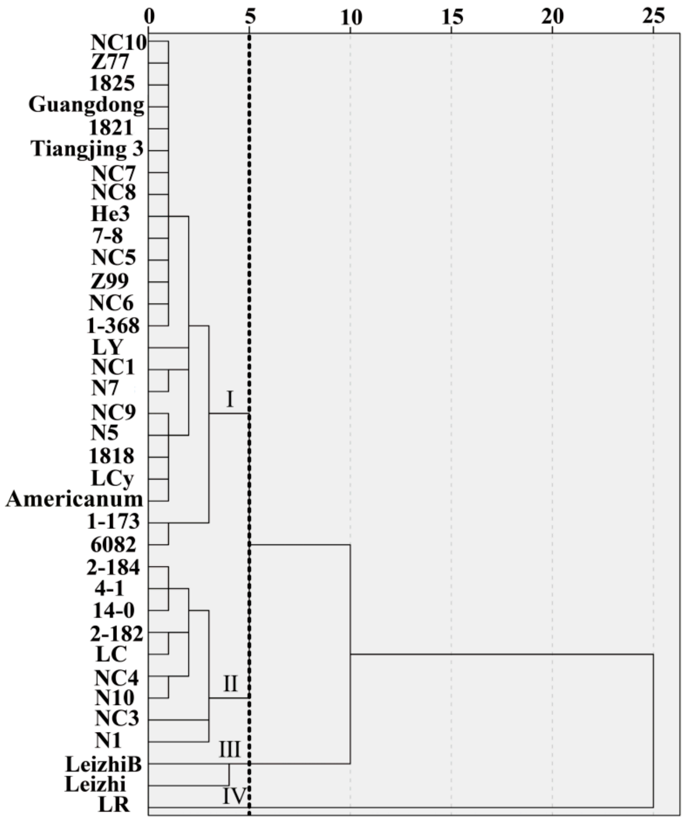

Figure 7. Cluster analysis of 36 goji germplasm resources. The designations I, II, III, IV signify that at a distance value of 5 (represented by the dashed line in the figure), the cultivars (lines) were categorized into four primary groups according to their similarity. The numerical identifiers for the 36 goji cultivars (lines) depicted in the figure correspond to the goji entries presented in Table 1.

3.4. Aceri Macrodonis Keifer Field Survey Experimental Results

By analyzing the average gall count (number of galls/number of leaves) and the infection area (total area of galls/total leaf area) in natural field infection settings, the resistance of different goji strains and variations to *A. pallida* was evaluated [22,23]. The findings (Figure 8) showed that different cultivars (lines) exhibited significant differences in their ability to withstand *A. pallida*, with the two metrics of the average number of galls per leaf and the ratio of infected area to total area producing results that were generally consistent. While N5 exhibited the highest sensitivity to *A. pallida*, Tianjing 3 showed the highest resistance, whereas the conventional N1 showed moderate resistance. The findings in this section align closely with the previous analysis regarding the wax proportion and its impact on stress resistance.

In the analysis of wax proportions, within the same 13 samples of goji used in the field experiment, Tianjing 3 exhibited the highest wax proportion, and N1 showed the lowest wax proportion. A greater wax content enhances the plant's resistance. The comprehensive resistance analysis revealed that N7 exhibited a higher resistance score, whereas 1-173 recorded the lowest score. The scoring outcomes were generally consistent with the results from the field experiments. The examination of the relationship between the average number of galls and the extent of infestation revealed a noteworthy correlation between the area affected by galls and the average count of galls present (Supplementary Table S3).

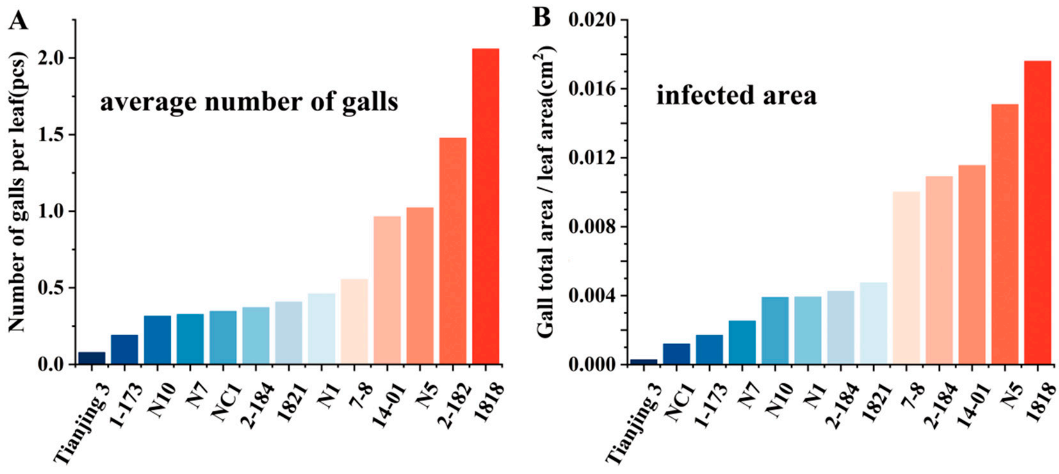

Figure 8. Field survey and experimental structural analysis of *A. pallida* galls. (**A**), Average Number of galls, where the *y*-axis shows the ratio of the number of *A. pallida* galls to the number of leaves; (**B**), Infected area, where the *y*-axis shows the ratio of the total area of *A. pallida* galls to the total area of the leaves. The *x*-axis of the graph represents several goji strains. The abbreviations for the goji cultivars (lines) in the graph align with the goji strains enumerated in Table 1.

4. Discussion

4.1. Relationship Between Leaf Anatomy and Drought Resistance

Leaves serve as highly sensitive organs in plants, capable of detecting alterations in the external environment. Their responses to various stresses are complex and involve interactions across multiple structural levels [24]. The anatomical characteristics of leaves effectively indicate a plant's capacity to adapt to spatiotemporal environmental variations [25]. Drought, cold damage, and pest infestation are significant environmental conditions that restrict crop development. The assessment and selection of resources exhibiting robust drought, cold, and pest tolerance is fundamental to the development of novel cultivars (lines) of goji [26,27]. Thicker leaves and epidermal cells improve a plant's water storage capacity and enhance its drought resistance [28]. Research examining the anatomical makeup of tobacco leaves has revealed that drought considerably thickens tobacco leaves [29]. Under conditions of moderate and severe drought stress, the leaf thickness of Camellia oleifera exhibited a significant decline [30]. This suggests a correlation between plant leaf thickness and variables including plant species, duration of stress treatments, and stress intensity. The cuticle on the leaf epidermis exhibits low permeability to water, thereby effectively reducing moisture evaporation and minimizing mechanical damage to the leaves, contributing to the water retention capacity of plant leaves [31]. The palisade tissue can adjust to variations in light intensity, thereby protecting the mesophyll cells of the plant from potential scorching damage caused by excessive sunlight. Previous studies on the selection of drought resistance evaluation indicators for Populus identified several typical indicators for the anatomical analysis of goji cultivars (lines). These indicators include upper epidermis thickness, palisade tissue, thickness of the upper and lower cuticles, palisade/spongy tissue ratio, and leaf tissue compactness [32]. There are notable differences in drought resistance among cultivars (lines) of goji germplasm, as evidenced by the analysis of the average membership function of six anatomical indicators in goji. LR and LCy were found to have a stronger overall drought resistance, while NC5 and 6082 had a lower drought resistance. The palisade tissue of NC5 and 6082 was discovered to be thinner than that of LR and LCy, which may be the cause of their varying drought tolerance. Furthermore, it was found that, in line with the results of earlier investigations, the drought resistance of goji is strongly correlated with the thickness of the upper epidermis, lower cuticle, and leaf tissue compactness (palisade/leaf thickness).

4.2. Relationship Between Leaf Anatomical Structure and Cold Resistance

The investigation of leaf anatomical structures in plants including *Magnoliaceae Juss*, *Michelia figo* (Lour.) Spreng, *Ziziphus jujuba* var, *Pyrus* spp., and *Taxus wallichiana* var. chinensis revealed a correlation between cold resistance and leaf anatomy. Specifically, varieties exhibiting greater cold resistance demonstrated thicker palisade tissue and increased leaf tissue compactness, which contribute to reduced damage from low temperatures and improved capacity to mitigate low temperature stress [33–37]. In the study of grapevines, a positive correlation was observed between the thickness of spongy tissue and cold resistance across various varieties, whereas palisade tissue exhibited minimal influence on cold resistance [38]. The indicators of plant leaf anatomical structure correlate with environmental adaptability; a thicker palisade tissue is associated with increased chloroplast content. The plant leaf serves as the primary location for the exchange of substances and energy with the external environment, and a correlation exists between leaf microstructure and stress resistance [39]. The leaf is shielded from pathogen infection, water loss through transpiration, and interference from intense solar radiation by the cuticle layer, which is rich in cuticle polymers and waxes and is found on the outermost surface of the epidermis. The thickness of the epidermis and cuticle in most woody plants correlates directly with the plant's tolerance to drought and cold conditions. Yin et al. demonstrated that the upper epidermis of the leaf offers greater protection compared to the lower epidermis. A thicker upper epidermis and cuticle enhance a plant's capacity to withstand high temperatures, drought, low temperatures, and biotic stress [39]. The palisade tissue, situated beneath the upper epidermis, exhibits increased thickness and development, resulting in enhanced photosynthetic activity and improved water use efficiency in the leaf [40]. It collaborates with the upper epidermis to shield the underlying mesophyll tissue from damage caused by intense light, thereby enhancing the plant's drought resistance [41]. The palisade tissue also influences the cold resistance of goji. The reduced intercellular spaces and lower water content in palisade tissue effectively mitigate damage to leaf tissue caused by the freezing of intercellular water in low-temperature environments. The thickness and layering of palisade tissue correlate positively with the plant's cold resistance [42]. The calculation of cold resistance scores for goji, utilizing the average membership function across six indicators, revealed significant differences in cold resistance among various goji germplasm resources. The highest rankings were attributed to LR and LCy. This result indicates a minor variation in the drought resistance strength among goji resources, implying that the contribution of distinct traits within the same leaf anatomical structure to managing different environmental stresses is not markedly different.

4.3. Relationship Between Leaf Anatomical Structure and Insect Resistance

Plant features such as structure, color, waxy layers, epidermal and glandular hairs, as well as the size and distribution of stomata, are effective in preventing pests. For example, insect-resistant cotton flower varieties are less pest resistant than common varieties [43]. Moreover, leaf morphology, physiological characteristics, and wax content are closely related to plant mite resistance. Field studies showed that the number of stomata in the lower eggplant epidermis was highly positively correlated with the density of a species of mite, but not on the leaf surface [44]. Plant morphology and structure are closely related to insect resistance, which not only reveals the physical interaction between pests and plants, but also provides a practical method for insect resistance breeding and biological control [45]. The leaf waxy layer is essential for maintaining water and protection against pathogens and small spiny insects [46]. It is found that the thicker the leaf waxy layer, the higher the content, the stronger the keratinization, the more difficult the feeding of mites, and the stronger the anti-mite resistance of the plant [47–49]. Studies on the anatomical structures of mulberry, tea, and maple trees indicate that types exhibiting greater insect resistance typically possess thicker palisade tissue, spongy tissue, and both upper and lower epidermis [50–52]. Investigations have identified an association between the density and size of stomata and the resilience of crop cultivars. Zhou discovered that the stomata on the lower epidermis of sugarcane leaves in the rib region are diminutive and closely packed, which hinders the feeding damage caused by the sugarcane aphid and is a primary reason for sugarcane's resistance to the cotton aphid [53]. An examination of 13 anatomical features across several goji cultivars (lines) revealed that LR and LCy possess thicker palisade and spongy tissues than the other 34 goji cultivars (lines) examined. LR and LCy are positioned as the top two for insect resistance among the 36 different cultivars (lines) of goji germplasm resources. The examination of the leaf stomata of goji germplasm revealed that LCy possesses the smallest stomatal opening, potentially correlating with its insect resistance. The examination of wax content revealed that LR and LCy occupy the top two positions for wax proportion, indicating a potential correlation between wax content and their resistance to insects.

5. Conclusions

This experiment involved the analysis of 13 anatomical traits of goji germplasm resources to assess their resistance. Informed by prior research, we employed six indicators for our analysis: thickness of the upper epidermis, thickness of the palisade tissue, leaf thickness, thickness of spongy tissue, thickness of the lower cuticle, and Palisade tissue thickness/total leaf thickness compactness to assess insect resistance in goji; thickness of the upper epidermis, thickness of the palisade tissue, leaf thickness, thickness of the upper cuticle, thickness of the lower cuticle, and palisade tissue thickness/spongy tissue thickness compactness for evaluating cold resistance; and thickness of the upper epidermis, thickness of the palisade tissue, thickness of the upper cuticle, thickness of the lower cuticle, leaf thickness, and palisade tissue thickness/total leaf thickness for examining drought resistance in goji. Furthermore, we conducted an analysis of the stomatal conditions, wax content, and the outcomes of *A. pallida* infection across 13 goji cultivars (lines) in the field. The analysis of various goji resistances revealed that thickness of the upper cuticle and thickness of the lower cuticle exhibited a stronger correlation with resistance, suggesting that these two indicators may serve as more effective predictors of goji resistance. The stomatal analysis indicated variations in stomatal density and aperture across various goji strains, with their stomatal characteristics correlating to their resistance. The examination of the leaf wax layer indicated that Tianjing 3 possesses a greater proportion of wax content. Furthermore, the results from the field experiment regarding *A. pallida* infection indicated that Tianjing 3 exhibited the lowest infection levels. The degree of infection across the 13 goji varieties in the field experiment was largely consistent and correlated with their wax content, suggesting a relationship between leaf wax content and resistance to *A. pallida*. The findings from the membership function and principal component analysis indicated that, among the 36 goji germplasm resources, LR and LCy exhibited the highest overall resistance. The research findings offer valuable insights for the selection and breeding of goji germplasm resources.

Supplementary Materials: The following supporting information can be downloaded at: https://www.mdpi.com/article/10.3390/f16010187/s1. Table S1: The characteristics of the goji leaves' anatomical structure index vary widely. Table S2: Stomatal characteristics of the tested goji cultivars (lines). Table S3: Field survey and experimental structural analysis of *A. pallida*.

Author Contributions: Conceptualization, Z.Y. and C.W.; methodology, Z.Y. and C.W.; software, Z.Y. and C.W.; investigation, Z.Y., J.W. and Z.W., resources, G.D. and K.Q.; data curation, C.W.; writing—original draft preparation, Z.Y.; writing—review and editing, Z.Y. and C.W.; supervision, C.W.; project administration, C.W.; funding acquisition, C.W. All authors have read and agreed to the published version of the manuscript.

Funding: This research was funded by Natural Science Foundation of Ningxia, grant number 2023AAC03314; National Natural Science Foundation of China, grant number 32460731; Research and Development Project of Ningxia Hui Autonomous Region, grant number 2021BEF02005; West Light Talent Program of the Chinese Academy of Sciences, grant number XAB2022YW08; and Graduate Innovation and Entrepreneurship Program of North Minzu University, grant number YCX24408.

Data Availability Statement: The datasets supporting the results presented in this manuscript are included within the article (and its Supplementary Materials).

Conflicts of Interest: The authors declare no conflicts of interest.

References

1. Ryu, T.H.; Kang, C.Y.; Jung, Y.B.; Ko, N.Y.; Kwon, H.R.; Seo, M.J.; Yu, Y.M.; Youn, Y.N.; Kim, Y.G. Occurrence patterns of insect pests in the field of *Lycium chinense* under environment-friendly management. *Korean J. Agric. Sci.* **2014**, *41*, 341–350. [CrossRef]
2. Xu, C.Q.; Liu, S.; Xu, R.; Chen, J.; Cheng, H.Z. Investigation of production status in major *Lycium barbarum* producing areas of China and some suggestions. *China J. Chin. Mat. Med.* **2014**, *39*, 1979–1984.
3. Xie, J.; Tang, W.; Jin, M.; Li, J.E.; Xie, M.Y. Recent advances in bioactive polysaccharides from *Lycium barbarum*, *Zizyphus jujuba* Mill., *Plantago* spp., and *Morus* spp.: Structures and functionalities. *Food Hydrocoll.* **2016**, *60*, 148–160. [CrossRef]
4. Atanasova, D.Y.; Semerdjieva, I.B. Population density of *Phytonomus variabilis* hrbst. and *Phytodecta fornicata* brugg on multifoliolate and trifoliolate alfalfa in relation to anatomical characteristics on their leaves. *J. Cent. Eur. Agric.* **2009**, *10*, 321–326.
5. Nie, S.; Mo, S.; Gao, T.; Bing, Y.; Shen, P.; Kashif, M.; Zhang, Z.; Li, J.; Jiang, C. Coupling effects of nitrate reduction and sulfur oxidation in a subtropical marine mangrove ecosystem with *Spartina alterniflora* invasion. *Sci. Total Environ.* **2023**, *862*, 160930. [CrossRef] [PubMed]
6. Ying, Y.X.; Xiao, Y.B.; Cui, W.Z.; Tan, Q.; Li, Y.; Luo, Y.; Wu, L.; Chen, F.; Li, C.; Ran, C. Spring photosynthetic phenology of Chinese vegetation in response to climate change and its impact on net primary productivity. *Agric. Meteorol.* **2023**, *342*, 109734.
7. Oliveira, A.F.; de Paula, M.S.; Cruz, M.C.; Almeida, M.O. Response to paclobutrazol application and water deficit on leaf anatomy of two olive tree cultivars. *Acta Hortic.* **2014**, *1057*, 51–56. [CrossRef]
8. Yan, Z.; Ma, T.; Guo, S.; Liu, R.; Li, M. Leaf anatomy, photosynthesis and chlorophyll fluorescence of lettuce as influenced by arbuscular mycorrhizal fungi under high temperature stress. *Sci. Hortic.* **2021**, *280*, 109933. [CrossRef]
9. Shen, H.F.; Zhao, B.; Xu, J.J. Relationship between leaf anatomical structure and heat resistance of 15 *Rhododendron* cultivars. *J. Appl. Ecol.* **2016**, *27*, 3895–3904.
10. Li, R.X.; Jin, X.L.; Hu, X.J.; Chai, X.Y.; Cai, M.Y.; Luo, F.; Zhang, F. Analysis and comprehensive evaluation on cold resistance of six varieties of *Michelia*. *J. South China Agric. Univ.* **2017**, *28*, 1464–1472.
11. Guo, X.M.; Liu, J.Z.; Zhai, J.T.; Xiao, X.; Lu, Y.; Li, D.; Pei, S.; Zhang, L. The relationship between leaf anatomical structure and cold resistance of 16 peach varieties. *For. Sci.* **2015**, *51*, 33–43.
12. Ladyzhenko, T. Leaf anatomical structure of *Nerium oleander* L. as a reflection of its adaption potential on habitat. *Mod. Phytomorphol.* **2014**, *6*, 197–200.
13. Salsinha, Y.C.F.; Maryani; Indradewa, D.; Purwestri, Y.A.; Rachmawati, D. Leaf physiological and anatomical characters contribute to drought tolerance of *Nusa tenggara* Timur local rice cultivars. *J. Crop. Sci. Biotechnol.* **2021**, *24*, 337–348. [CrossRef]
14. Olbricht, K.; Ludwig, A.; Ulrich, D.; Spangeberg, R.; Guenther, M.; Neinhuis, C. Leaf morphology and anatomy in the genus *Fragaria*: Implications for resistances. *Acta Hortic.* **2014**, *1049*, 269–273. [CrossRef]
15. Hu, Y.; Yang, L.; Gao, C.; Liao, D.C.; Long, L.; Qiu, J.; Wei, H.; Deng, Q.; Zhou, Y. A comparative study on the leaf anatomical structure of *Camellia oleifera* in a low-hot valley area in Guizhou Province, China. *PLoS ONE* **2022**, *17*, e0262509. [CrossRef] [PubMed]
16. *TB 852-2023*; Goji Technical Procedures for Monitoring and Forecasting Diseases and Pests. Ningxia Hui Autonomous Region Market Supervision and Administration Department: Ningxia, China, 2023.
17. Hetherington, A.M.; Woodward, F.I. The role of stomata in sensing and driving environmental change. *Nature* **2003**, *424*, 901–908. [CrossRef]
18. Quan, Q.; Xin, P.; Li, J.Y.; Wang, J.H.; Kun, A.D. Morphological traits and physiological characteristics in drought tolerance in 20 shrub species on the Qinghai-Xizang *Plateau*. *Chin. J. Plant Ecol.* **2014**, *38*, 562–575. [CrossRef]

19. Wang, Q.S.; Huang, J.; Chen, C.S.; Wu, G.Y.; Zeng, M.S.; Huang, C.M.; Chen, R.B. Relationship between leaf structure of tea germplasm and its resistance to *Aleurocanthus spiniferus* (Quaintance). *J. Tea Sci.* **2009**, *29*, 60–66.
20. Xu, H.; Huang, C.; Jiang, X.; Zhu, J.; Gao, X.; Yu, C. Impact of cold stress on leaf structure, photosynthesis, and metabolites in *Camellia* weiningensis and *C. oleifera* Seedling. *Acta Hortic.* **2022**, *8*, 494. [CrossRef]
21. Kerstiens, G. Plant cuticles-an integrated functional approach. *J. Exp Bot.* **1996**, *47*, 50–60. [CrossRef]
22. Post-Beittenmiller, D. Biochemistry and molecular biology of wax production in plants. *Annu. Rev. Plant Physiol. Plant Mol. Biol.* **1996**, *47*, 405–430. [CrossRef] [PubMed]
23. Fei, S.L.; Fang, J.Y.; Fan, Y.J.; Zhao, K.; Cui, K.M. Anatomical characteristics of leaves and woods of *Fagus lucida* and their relationship to ecological factors in Mountain Fanjingshan, Guizhou, China. *Acta. Sin.* **1999**, *41*, 1002–1009.
24. Zivcak, M.; Brestic, M.; Balatova, Z.; Drevenakova, P. Photosynthetic electron transport and specific photoprotective responses in wheat leaves under drought stress. *Photosyn. Res.* **2013**, *117*, 529–546. [CrossRef] [PubMed]
25. Chaves, M.M.; Flexas, J.; Pinheiro, C. Photosynthesis under drought and salt stress: Regulation mechanisms from whole plant to cell. *Ann. Bot.* **2009**, *103*, 551–560. [CrossRef] [PubMed]
26. Klich, M.G. Leaf variations in *Elaeagnus angustifolia* related to environmental heterogeneity. *Environ. Exp. Bot.* **2000**, *44*, 171–183. [CrossRef] [PubMed]
27. Huang, L.; Zhang, L.; Zeng, R.; Wang, X.; Zhang, H.; Wang, L.; Liu, S.; Wang, X.; Chen, T. Brassinosteroid priming improves *Peanut* drought tolerance via eliminating inhibition on genes in photosynthesis and hormone signaling. *Genes* **2024**, *11*, 919. [CrossRef]
28. Stremoukhov, O.; Koshovyi, O.M.; Gontova, T.; Komisarenko, M.A.; Borodina, N.V. Elemental composition, morphological and anatomical features of blueberry leaves. *Fitoterapia* **2020**, *1*, 50–57. [CrossRef]
29. Khan, R.; Ma, X.; Hussain, Q.; Chen, K.; Farooq, S.; Asim, M.; Ren, X.; Shah, S.; Shi, Y. Transcriptome and anatomical studies reveal alterations in leaf thickness under long-term drought stress in *tobacco*. *J. Plant Physiol.* **2023**, *281*, 153920. [CrossRef] [PubMed]
30. Yao, Y.; Nan, L.; Wang, K.; Xia, J.; Ma, B.; Cheng, J. Integrative leaf anatomy structure, physiology, and metabolome analyses revealed the response to drought stress in sainfoin at the seedling stage. *Phytochem. Anal. PCA* **2024**, *35*, 1174–1185. [CrossRef] [PubMed]
31. Bai, T.; Li, Z.; Song, C.; Song, S.; Jiao, J.; Liu, Y.; Dong, Z.; Zheng, X. Contrasting drought tolerance in two apple cultivars associated with difference in leaf morphology and anatomy. *Am. J. Plant Sci.* **2019**, *10*, 709–722. [CrossRef]
32. Jin, Y.; Zhao, X.; Liu, W.; Liang, G.; Zhang, Y. Germplasm resources and drought resistance evaluation of *Siberian wildrye* (*Elymus sibiricus* L.) in the Tibetan Plateau. *Braz. J. Bot.* **2023**, *46*, 743–756. [CrossRef]
33. Xie, T.W.; Ou, Y.M.S. Anatomy of the leaves and freezing hardiness of thirteen species of *Magnoliaceae*. *Plant Sci.* **1989**, *7*, 234–238.
34. Li, B.; Zhang, Y.; Kang, Y.; Wang, Y.; Liu, R.; Liu, Q.; Dong, S. Physiological response to low-temperature stress and cold resistance evaluation of *Ziziphus jujuba* var. spinosa clones from different provenances. *Forests* **2024**, *15*, 1130. [CrossRef]
35. Huan, L.; Li, G.; Ming, J.; Jin, X.; Li, L.; Hao, B. Evaluation of cold resistance and semi-lethal low temperature (LT50)of nine pear cultivars. *Asian J. Agric. Res.* **2024**, *16*, 45–47.
36. Chen, H.H.; Li, P.H. Interactions of low temperature, water stress, and short days in the induction of stem frost hardiness in red osier dogwood. *Plant Physiol.* **1978**, *62*, 833–835. [CrossRef] [PubMed]
37. Ma, Y.Y.; Zhang, Y.L.; Shao, H.; Liu, J. Differential physio-biochemical responses to cold stress of cold-tolerant and non-tolerant grapes (*Vitis* L.) from China. *J. Agron. Crop. Sci.* **2010**, *196*, 212–219. [CrossRef]
38. Rui, L. Examination of Anatomical structure of cocos *nucifera L.* leaf from different varieties. *Southwest China J. Agric. Sci.* **2011**, *24*, 1425–1429.
39. Yin, X.; Putten, P.; Belay, D.; Struik, P.C. Using photorespiratory oxygen response to analyse leaf mesophyll resistance. *Photosyn. Res.* **2020**, *144*, 85–99. [CrossRef] [PubMed]
40. Galmés, J.; Ochogavía, J.M.; Gago, J.; Roldán, E.J.; Cifre, J.; Conesa, M.À. Leaf responses to drought stress in Mediterranean accessions of *Solanum lycopersicum*: Anatomical adaptations in relation to gas exchange parameters. *Plant Cell Environ.* **2013**, *36*, 920–935. [CrossRef] [PubMed]
41. Ye, Y.R.; Wang, W.L.; Zheng, C.S.; Fu, J.; Liu, H.W. Evaluation of cold resistance of four wild *Carex* speices. *Chin. J. App. Ecol.* **2017**, *28*, 89–95.
42. Jie, Z.; Wei, H.; Li, Y.X.; He, J.Q.; Zhu, H.H.; Zhou, Z.G. Screening of drought resistance indices and evaluation of drought resistance in cotton (*Gossypium hirsutum* L.). *J. Integr. Agric.* **2020**, *19*, 495–508.
43. Bhusal, N.; Lee, M.; Lee, H.; Adhikari, A.; Kim, H.S. Evaluation of morphological, physiological, and biochemical traits for assessing drought resistance in eleven tree species. *Sci. Total Environ.* **2021**, *779*, 146466. [CrossRef] [PubMed]
44. Gupta, A.; Andres, R.M.; Cao-Delgado, A.I. The physiology of plant responses to drought. *Science* **2020**, *368*, 266–269. [CrossRef] [PubMed]

45. Gibadulina, I.I.; Larionov, M.V.; Maslennikova, N.N. Anatomical and morphological features of the leaves of *Tilia Cordata* Mill. As an Indicator of the Adaptive Capabilities of the species to the conditions of the urban environment. *IOP Conf. Ser. Earth Environ. Sci.* **2024**, *998*, 032082. [CrossRef]
46. Rubiales, D.; Khazaei, H. Advances in disease and pest resistance in faba bean. *Theor. Appl. Genet.* **2022**, *135*, 3735–3756. [CrossRef] [PubMed]
47. Shad, M.; Yasmeen, A.; Azam, S.; Bakhsh, A.; Latif, A.; Shahid, N.; Salah, U.D.; Sadaqat, S.; Rao, A.Q.; Shahid, A.A. Enhancing the resilience of transgenic cotton for insect resistance. *Mol. Biol. Rep.* **2021**, *49*, 5315–5323. [CrossRef] [PubMed]
48. Ferry, N.; Edwards, M.G.; Gatehouse, J.A.; Gatehouse, A.M. Plant–insect interactions: Molecular approaches to insect resistance. *Curr. Opin. Biotech.* **2004**, *15*, 155–161. [CrossRef] [PubMed]
49. Daud, R.D.; Elenicede, C.C.; Reinaldo, J.F.F. Changes in leaf physiology caused by *Calacarus heveae* (Acari, Eriophyidae) on rubber tree. *Exp. Appl. Acarol.* **2012**, *57*, 127–137. [CrossRef]
50. Radmila, P.; Kielkiewicz, M. Plant-eriophyoid mite interactions: Specific and unspecific morphological alterations. Part II. *Exp. Appl. Acarol.* **2010**, *51*, 81–91.
51. Wilson, L.J. Resistance of Okra-Leaf cotton genotypes to twospotted spider mites (Acari: *Tetranychidae*). *J. Econ. Entomol.* **1994**, *87*, 1726–1735. [CrossRef]
52. Macedo, T.B.; Peterson, R.K.D.; Weaver, D.K. Photosynthetic responses of wheat, *Triticum aestivum* L. plants to simulated insect defoliation during vegetative growth and at grain fill. *Environ. Entomol.* **2006**, *35*, 1702–1709. [CrossRef]
53. Juan, W.; Lin, L.; Xiang, X.; Yizhong, Y.; Wang, A. Physiological variation of damaged leaves of tomato by *Aculops* lycopersici. *Acta Hortic. Sin.* **2006**, *6*, 1215–1218.